A HIGHER-ORDER INTERNAL WAVE MODEL ACCOUNTING FOR LARGE BATHYMETRIC VARIATIONS

AILÍN RUIZ DE ZÁRATE*, DANIEL G. ALFARO VIGO†, ANDRÉ NACHBIN‡, AND WOOYOUNG CHOI §

Abstract.
A higher-order strongly nonlinear model is derived to describe the evolution of large amplitude internal waves over arbitrary bathymetric variations in a two-layer system where the upper layer is shallow while the lower layer is comparable to the characteristic wavelength. The new system of nonlinear evolution equations with variable coefficients is a generalization of the deep configuration model proposed by Choi and Camassa (Journal of Fluid Mechanics, 1999) and accounts for both a higher-order approximation to pressure coupling between the two layers and the effects of rapidly-varying bottom variation. Motivated by the work of Rosales and Papanicolaou (Studies Appl. Math., 1983), an averaging technique is applied to the system for weakly nonlinear long internal waves propagating over periodic bottom topography. It is shown that the system reduces to an effective Intermediate Long Wave (ILW) equation, in contrast to the KdV equation derived for the surface wave case.

Key words. Internal waves, Inhomogeneous media, Asymptotic theory, Effective media.

1. Introduction

Modeling internal waves is of great interest in the study of ocean and atmosphere dynamics. Large amplitude internal ocean waves, for example, are often observed in many areas where the variation of temperature and salt concentration generates density stratification. They can interact with bottom topography and submerged structures as well as surface waves. In particular, in oil recovery in deep oceans, these highly nonlinear internal waves can affect offshore operations and submerged structures. Another example, in the context of atmosphere dynamics, is the effect on the topographic form drag which is of importance in the study of pollution dispersion in an urban area.

Finding accurate reduced models is a first step toward better understanding the characteristics of large amplitude internal waves and developing efficient computational methods to solve a wide range of practical problems in the ocean and the atmosphere. To describe the nonlinear internal wave motions in water of great depth, various models have been proposed, ranging from classical weakly nonlinear models such as the Intermediate Long Wave (ILW) equation and the Benjamin-Ono (BO) equation [2, 9, 19, 20, 31] to high-order nonlinear models [4, 5, 6, 18, 23]. A strongly nonlinear long wave model of Choi and Camassa [6] for the deep configuration that is known to approximate well large amplitude internal solitary waves is of particular interest, but is valid only for the case of flat or slowly-varying bottom.

In this paper, for a two-layer fluid of finite depth, a higher-order nonlinear model is derived to study the interaction of nonlinear internal waves with large amplitude bottom topography that might vary rapidly over the characteristic length scale of internal waves. As shown in Fig. 2.1, two layers of constant densities are bounded by a horizontal rigid lid at the top and arbitrary topography at the bottom. The thickness of the lower layer is assumed to be much greater than that of the upper layer, but is comparable to the characteristic wavelength.

*Universidade Federal do Paraná, Centro Politécnico, Jardim das Américas, Curitiba, PR, Brazil, caixa postal 019081 CEP 81531-990 (ailinruizdezarate@gmail.com). The author was supported by an ANP/PRH-32 scholarship.

†Instituto de Matemática Pura e Aplicada, Estrada Dona Castorina 110, Jardim Botânico, Rio de Janeiro, RJ, Brazil, CEP 22460-320 (dgalfaro@impa.br). The author was supported by a CNPq scholarship through the Instituto do Milênio

‡Instituto de Matemática Pura e Aplicada, Estrada Dona Castorina 110, Jardim Botânico, Rio de Janeiro, RJ, Brazil, CEP 22460-320 (nachbin@impa.br). This work was supported by CNPq/Brazil under Grant 300368/96-8

§Dept. of Mathematical Sciences, New Jersey Institute of Technology, Newark, NJ 07102-1982 (wychoi@njit.edu). The author was supported by the US National Science Foundation through Grant No. DMS-0620832.

The new long wave model, accounting for higher-order nonlinear effects through a more accurate pressure coupling between the two layers, describes the evolution of the internal wave elevation together with the mean (horizontal) water velocity for the upper layer. The effects of rapidly-varying and steep topography are represented in the model by variable coefficients with the aid of the conformal mapping technique, as described in [29].

By using a multi-scale averaging strategy, Rosales and Papanicolaou [32] obtained an effective KdV equation for weakly nonlinear and weakly dispersive long surface waves over rapidly-varying and periodic bathymetry for which wave reflection is negligible. Other more recent results can be found in the literature [8, 16], all containing effective KdV equations. In the present work, the analysis is carried over for internal waves, with an additional technical difficulty of expanding a singular integral operator acting on a multi-scale function. Under the weakly nonlinear assumption, to leading order, it is shown that the higher-order model can be reduced to an effective ILW equation when considering unidirectional internal waves over rapidly-varying and periodic bathymetry.

We intend to use this higher-order model to study the interaction of internal waves with bottom topography, including topics such as wave multiple-scattering, and related interesting phenomena that arise. To mention a few, connected with our previous experience for surface waves, we have the apparent diffusion of long waves interacting with a random topography [10, 13, 14, 15, 24, 28], as well as the time reversal refocusing of pulses [11, 12, 25, 26], viewed as a tool for waveform inversion. Namely, from the scattered wave field one can reconstruct numerically the initial wave profile. Having the effective ILW model, for the periodic case, is a very useful tool in validating new numerical methods designed to capture long wave-microstructure interaction.

The paper is organized as follows. In Section 2, the physical setting is defined together with a brief description of our previous results. In Section 3, we introduce the higher-order, depth-averaged, upper layer equations that are equivalent to the shallow water equations with a leading-order dispersive term. Then, in Section 4, the lower layer pressure that brings in information from the bathymetry is expanded to the next-order term, in comparison with previous work. In Section 5, a new, higher-order, strongly nonlinear model is presented. Also its weakly nonlinear version is given. A dispersive analysis compares the new models with the (full) Euler equations. Finally, in Section 6, by considering a rapidly varying periodic bathymetry, a multi-scale averaging theory is presented and an effective Intermediate Long Wave (ILW) model is deduced. The conclusions are given in Section 7 while the appendix contains a proof for expanding the singular integral operator.

2. Physical setting

We start with a two-fluid configuration. The coordinate system is positioned at the undisturbed interface between two layers. The displacement of the interface is denoted by $\eta(x,t)$ and we assume that it is smooth and has compact support. See Fig. 2.1. The density of each inviscid, immiscible, incompressible and irrotational fluid is ρ_1 for the upper fluid and ρ_2 for the lower fluid. For a stable stratification, let $\rho_2 > \rho_1$. Similarly, (u_i, w_i) denote the velocity components and p_i the pressure, where $i = 1, 2$. The upper layer is assumed to have a characteristic thickness of h_1, much smaller than the characteristic wavelength L at the interface. Hence, the upper layer will be in the shallow water regime. At the lower layer, the irregular bottom is described by $z = h_2(h(x/l) - 1)$, $h < 1$. The function h can be discontinuous or even multivalued. See, for example, Fig. 2.1 where a polygonal shaped topography is sketched. Moreover, the characteristic depth for the lower layer h_2 is comparable with the characteristic wavelength L, hence, characterizing an intermediate depth regime. When a rapidly varying bottom is taken into account, the horizontal length scale for bottom irregularities l is such that $h_1 < l \ll L$. In this work, subscripts ξ, x, z and t stand for partial derivatives with respect to

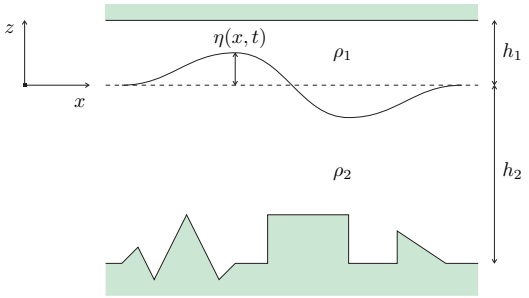

FIG. 2.1. *Two-fluid system configuration.*

spatial coordinates and time.

Introducing the nondimensional dispersion parameter $\beta=(h_1/L)^2$, it follows from the shallowness of the upper layer that $O\left(\sqrt{\beta}\right)\ll 1$. The physical variables regarding the upper layer are nondimensionalized (with a tilde) as follows [6, 29]:

$$x=L\tilde{x}, \qquad z=h_1\tilde{z}, \qquad t=\frac{L}{U_0}\tilde{t}, \qquad \eta=h_1\tilde{\eta},$$
$$p_1=(\rho_1 U_0^2)\tilde{p}_1, \qquad u_1=U_0\tilde{u}_1, \qquad w_1=\sqrt{\beta}U_0\tilde{w}_1,$$

where $U_0=\sqrt{gh_1}$ is the characteristic shallow layer speed. In a weakly nonlinear theory, η is usually scaled by a small characteristic amplitude a such that $\alpha\equiv a/h_1\ll 1$. Notice that here η is of the same order as the layer's depth. This will lead to a strongly nonlinear model.

For the lower layer, the intermediate depth regime implies $h_2/L=O(1)$ and, therefore, the nondimensionalization should be different [6, 29]:

$$x=L\tilde{x}, \qquad z=L\tilde{z}, \qquad t=\frac{L}{U_0}\tilde{t}, \qquad \eta=h_1\tilde{\eta},$$
$$p_2=(\rho_1 U_0^2)\tilde{p}_2, \qquad u_2=\sqrt{\beta}U_0\tilde{u}_2, \qquad w_2=\sqrt{\beta}U_0\tilde{w}_2,$$

together with the velocity potencial $\phi=\sqrt{\beta}U_0L\tilde{\phi}$.

One starts with the Euler equations in both (upper and lower) layers, together with a rigid lid condition at the top of the upper layer and an impermeability condition at the irregular bottom topography. Also one has continuity conditions at the interface: namely, a kinematic condition at the interface together with no pressure jumps. Considering the shallow water regime for the upper layer together with potential theory for the lower layer, the following reduced model arises from these Euler equations. This asymptotic reduction makes use of a terrain-following horizontal coordinate ξ [27] and was obtained in [29]:

$$\begin{cases} \eta_t-\dfrac{1}{M(\xi)}\left[(1-\eta)u\right]_\xi=0, \\ u_t+\dfrac{1}{M(\xi)}u\,u_\xi+\dfrac{1}{M(\xi)}\left(1-\dfrac{\rho_2}{\rho_1}\right)\eta_\xi=\sqrt{\beta}\dfrac{\rho_2}{\rho_1}\dfrac{1}{M(\xi)}\mathcal{T}_h\left[((1-\eta)u)_{\xi t}\right]. \end{cases} \tag{2.1}$$

This is a variable coefficient Boussinesq-type system for the internal wave profile η and the upper depth-averaged velocity u. The variable coefficient $M(\xi)$ has information from the topography, due to the conformal mapping of a flat strip onto the lower fluid domain [27, 29]. The map goes from (ξ,ζ) to (x,z) coordinates. Then, one can write the Jacobian along the

undisturbed interface as $|J|(\xi,0) = z_\xi(\xi,0)^2 \equiv M(\xi)^2$. As will be shown below, system (2.1) is a dispersive model, where dispersion comes in through the term with a Hilbert transform on a strip (of width h) given by

$$\mathcal{T}_h[f](\xi) \equiv \frac{1}{2h} \fint f(\tilde{\xi}) \coth\left(\frac{\pi}{2h}(\tilde{\xi}-\xi)\right) d\tilde{\xi}. \tag{2.2}$$

The singular integral must be interpreted as a Cauchy principal value. If the bottom is flat, $M(\xi) = 1$ and we obtain the same system derived by Choi and Camassa [6] for the deep configuration.

3. Higher-order upper layer equations We are interested in wave interaction with large amplitude topographies. Therefore, our reduced model must be able to account for a higher-order pressure coupling between the two layers. In other words, we want to investigate when this higher-order term does indeed play a role in the dynamics. Hence, our goal in this section is to improve the order of approximation of system (2.1) by computing a more accurate approximation for the pressure term: instead of an order β approximation, we include the next-order term of $O(\beta^{3/2})$.

We start with the layer-mean equations for the upper fluid ([34, 3, 6, 30]). For convenience, they are repeated here:

$$\eta_t - ((1-\eta)u)_x = 0, \tag{3.1}$$

$$u_t + uu_x = -\overline{p_{1x}} + O(\beta^2), \tag{3.2}$$

where $\overline{p_{1x}}$ is the mean-layer value for p_{1x}. For a better approximation of $\overline{p_{1x}}$, we need to expand $p_1(x,z,t)$ with one more term: $p_1(x,z,t) = p_1^{(0)} + \beta p_1^{(1)} + O(\beta^2)$, so its vertical derivative is expanded as $p_{1z}(x,z,t) = p_{1z}^{(0)} + \beta p_{1z}^{(1)} + O(\beta^2)$. From the vertical (Euler) momentum equation, we have $p_{1z} = -1 - \beta(w_{1t} + u_1 w_{1x} + w_1 w_{1z})$. We clearly see the $O(1)$ hydrostatic contribution to the pressure ($p_{1z}^{(0)} = -1$) together with a nonhydrostatic correction $p_{1z}^{(1)} = -(w_{1t}^{(0)} + u_1^{(0)} w_{1x}^{(0)} + w_1^{(0)} w_{1z}^{(0)})$. Again continuity of pressure at the interface ($p_1 = p_2$) enables the calculation of the leading-order nonhydrostatic correction arising from the lower layer. After some manipulations and asymptotics with the Euler equations along the upper layer, Choi and Camassa [6] describe a pressure approximation in a compact format: $p_{1z}^{(1)} = (z-1)G_1(x,t) + O(\beta)$, where $G_1(x,t) = u_{xt} + uu_{xx} - u_x u_x$. Integrating the expression for p_1 with respect to z from $z = \eta(x,t)$, differentiating once in x, and depth-averaging leads to

$$\overline{p_{1x}} = \eta_x + P_x(x,t) - \frac{\beta}{\eta_1}\left(\frac{1}{3}\eta_1^3 G_1(x,t)\right)_x + O(\beta^2), \tag{3.3}$$

where $\eta_1 = 1 - \eta$ and $P(x,t) = p_1(x,\eta(x,t),t) = p_2(x,\eta(x,t),t)$. Substituting (3.3) in (3.2), we have

$$u_t + uu_x = -\left(\eta_x + P_x(x,t) - \frac{\beta}{\eta_1}\left(\frac{1}{3}\eta_1^3 G_1(x,t)\right)_x\right) + O(\beta^2). \tag{3.4}$$

One can establish the following interesting connection with well known water wave models [6]. If the lower fluid layer is neglected and P is regarded as the external pressure applied to the free surface, Eqs. (3.1) and (3.4) are the complete set of evolution equations for surface waves as derived by Su and Gardner [33] and independently by Green and Naghdi [17]. One should note that having the rigid lid at the top and the free surface (interface) below it, the connection between models is established by reflecting the present one about the x-axis, namely when gravity is considered reversed.

4. Improved approximation for the pressure at the interface

Now we show how an order $O(\beta^{3/2})$ approximation arises for $P_x(x,t) = \left(p_2(x,\eta(x,t),t)\right)_x$ from the (lower layer) Euler equations. The $\beta^{1/2}$ factor comes from the scaling in the lower layer.

In nondimensional variables, the lower Bernoulli law at the interface is

$$P(x,t) = -\frac{\rho_2}{\rho_1}\left(\sqrt{\beta}\phi_t + \frac{\beta}{2}(\phi_x^2+\phi_z^2) + \eta + C(t)\right)\Big|_{z=\sqrt{\beta}\,\eta(x,t)}.$$

By expanding in a Taylor series about $z=0$, we obtain that

$$P(x,t) = -\frac{\rho_2}{\rho_1}\left[\eta + \sqrt{\beta}\left(\phi_t|_{z=0} + \sqrt{\beta}\eta\,\phi_{tz}|_{z=0}\right) + \frac{\beta}{2}\left(\phi_x^2\big|_{z=0} + \phi_z^2\big|_{z=0}\right) + C(t)\right] + O(\beta^{\frac{3}{2}}). \tag{4.1}$$

From the kinematic condition

$$\phi_z = \eta_t + \sqrt{\beta}\eta_x\phi_x, \tag{4.2}$$

we have that $\phi_z = \eta_t + O\left(\sqrt{\beta}\right)$ at $z = \sqrt{\beta}\eta(x,t)$. It then follows that $\phi_z|_{z=0} = \eta_t + O\left(\sqrt{\beta}\right)$ and $\phi_{tz}|_{z=0} = \eta_{tt} + O\left(\sqrt{\beta}\right)$. Substituting in (4.1) leads to

$$P(x,t) = -\frac{\rho_2}{\rho_1}\left[\eta + \sqrt{\beta}\,\phi_t|_{z=0} + \beta\eta\eta_{tt} + \frac{\beta}{2}\left(\phi_x^2\big|_{z=0} + \eta_t^2\right) + C(t)\right] + O(\beta^{\frac{3}{2}}).$$

Notice that all quantities are evaluated at $z=0$; therefore, taking x-derivatives, we obtain:

$$P_x(x,t) = -\frac{\rho_2}{\rho_1}\left[\eta_x + \sqrt{\beta}\,\phi_{tx}|_{z=0} + \beta\left(\eta\eta_{tt} + \frac{1}{2}\eta_t^2 + \frac{1}{2}\,\phi_x^2\big|_{z=0}\right)_x\right] + O(\beta^{\frac{3}{2}}). \tag{4.3}$$

In the previous work (c.f. (2.16) in [29]), $P_x(x,t)$ was computed only up to the $O(\sqrt{\beta})$ term, so that it was enough to approximate $\phi_x|_{z=0}$ up to order $\sqrt{\beta}$. In the higher-order pressure expression (4.3) this calculation can still be used to approximate $\phi_x^2|_{z=0}$. We recall that in [29], we were able to express $\phi_x|_{z=0}$ in terms of the Hilbert transform on the strip $\mathcal{T}_h[f](\xi)$, where $h = h_2/L$. In other words we found that

$$\phi_x|_{z=0} \equiv \phi_x(x(\xi,0),0,t) = \frac{1}{M(\xi)}\mathcal{T}_h\left[M(\tilde{\xi})\eta_t(x(\tilde{\xi},0),t)\right](\xi) + O\left(\sqrt{\beta}\right) \tag{4.4}$$

where the time independent metric coefficient $M(\xi)$ is a smooth function [27, 29]. We also call attention to the fact that by using the Hilbert transform we are keeping the **full dispersive** nature of the lower layer potential theory problem. This will become evident in the next section.

In order to approximate the $O(\beta^{1/2})$ term in (4.3), it becomes necessary to obtain a higher-order approximation for $\phi_{tx}|_{z=0}$, namely up to order β, in contrast with (4.4). Again we can restrict our analysis to a linear (lower layer) potential theory problem having an undisturbed interface. There, the velocity potential satisfies an upper Neumann boundary condition (in $\phi_z|_{z=0}$), which will be determined up to order β. This is done through the kinematic condition at the free interface.

Taking the nonlinear kinematic condition (4.2) and subsituting the Taylor expansion $\phi_z\left(x,\sqrt{\beta}\eta\right) = \phi_z(x,0) + \sqrt{\beta}\eta\phi_{zz}(x,0) + O(\beta)$, we have $\phi_z(x,0) = \eta_t + \sqrt{\beta}\eta_x\phi_x(x,0) + \sqrt{\beta}\eta\phi_{xx}(x,0) + O(\beta)$, where the Laplace equation has been used. Then this is the same as

$$\phi_z(x,0) = \eta_t + \sqrt{\beta}(\eta\phi_x(x,0))_x + O(\beta). \tag{4.5}$$

Substituting (4.4) in (4.5) and observing that along the undisturbed interface $\partial_\xi = M(\xi)\partial_x$, we have that

$$\phi_z(x,0) = \eta_t + \frac{\sqrt{\beta}}{M(\xi)}\left(\eta \frac{1}{M(\xi)}\mathcal{T}_h[M(\tilde{\xi})\eta_t]\right)_\xi + O(\beta).$$

Also noting that $\phi_\zeta(\xi,0) = M(\xi)\,\phi_z(x(\xi,0),0)$ and $\mathcal{T}_h[\phi_\zeta(\xi,0)] = \phi_\xi(\xi,0)$, we arrive at

$$\phi_x(x,0) = \frac{1}{M(\xi)}\phi_\xi(\xi,0) = \frac{1}{M(\xi)}\mathcal{T}_h\left[M(\tilde{\xi})\eta_t + \sqrt{\beta}\left(\eta \frac{1}{M(\tilde{\xi})}\mathcal{T}_h[M(\xi')\eta_t]\right)_\xi\right] + O(\beta).$$

From

$$\phi_{tx}(x,0) = \frac{1}{M(\xi)}\mathcal{T}_h\left[M(\tilde{\xi})\eta_t + \sqrt{\beta}\left(\eta \frac{1}{M(\tilde{\xi})}\mathcal{T}_h[M(\xi')\eta_t]\right)_\xi\right]_t + O(\beta),$$

together with (3.1), $\eta_{tt} = ((1-\eta)u)_{xt} = ((1-\eta)u)_{\xi t}/M(\xi)$, we have

$$\sqrt{\beta}\,\phi_{tx}|_{z=0} = \frac{\sqrt{\beta}}{M(\xi)}\mathcal{T}_h\left[((1-\eta)u)_{\xi t}\right] + \frac{\beta}{M(\xi)}\mathcal{T}_h\left[\frac{\eta}{M(\xi)}\mathcal{T}_h\left[((1-\eta)u)_\xi\right]\right]_{\xi t} + O(\beta^{\frac{3}{2}}),$$

which is the higher-order expression we were seeking. Note that the Hilbert transform iterate is the (new) correction term. It is our future goal to understand the role of this $O(\beta)$ term in the internal wave/topography dynamics.

Summarizing, the higher-order pressure term connecting the top and lower layer is

$$P_x(x,t) = -\frac{\rho_2}{\rho_1}\left(\eta_x + \frac{\sqrt{\beta}}{M(\xi)}\mathcal{T}_h\left[((1-\eta)u)_{\xi t}\right] + \frac{\beta}{M(\xi)}\mathcal{T}_h\left[\frac{\eta}{M(\xi)}\mathcal{T}_h\left[((1-\eta)u)_\xi\right]\right]_{\xi t} + \right.$$
$$\left. \frac{\beta}{2M(\xi)}\left(\left\{\frac{1}{M(\xi)}\mathcal{T}_h\left[((1-\eta)u)_\xi\right]\right\}^2\right)_\xi + \frac{\beta}{M(\xi)}\left(\eta\eta_{tt} + \frac{1}{2}\eta_t^2\right)\right) + O(\beta^{\frac{3}{2}}).$$

This additional order of approximation is compatible with the nonhydrostatic/weakly dispersive correction added to the upper shallow water layer model (c.f. $O(\beta)$ term in (3.4)). It is also relevant to comment that compositions of the Hilbert operator $\mathcal{T}_h$ arises not only in this case, but also in the fully dispersive Boussinesq model obtained by Matsuno [22], Artiles and Nachbin [1] or Craig and Sulem [7] for surface gravity waves. In these references the authors were expanding Dirichlet-to-Neumann (DtN) operators about the undisturbed free surface.

In the next section, we perform a Fourier dispersion analysis of these models.

5. The higher-order strongly nonlinear model

Consider system (3.1) and (3.4) in curvilinear coordinates

$$\begin{cases} \eta_t = \dfrac{1}{M(\xi)}((1-\eta)u)_\xi, \\ \\ u_t + \dfrac{1}{M(\xi)}u\,u_\xi = -\dfrac{1}{M(\xi)}\eta_\xi + \dfrac{\beta}{(1-\eta)}\dfrac{1}{3M(\xi)}((1-\eta)^3 G_1)_\xi - P_x + O(\beta^2), \end{cases}$$

where G_1 in curvilinear coordinates reads,

$$G_1(\xi,t) = \frac{1}{M(\xi)}u_{\xi t} + \frac{u}{M(\xi)}\left(\frac{1}{M(\xi)}u_\xi\right)_\xi - \frac{1}{M(\xi)^2}u_\xi u_\xi.$$

With the higher-order pressure, the strongly nonlinear model becomes

$$\begin{cases} \eta_t = \dfrac{1}{M(\xi)}((1-\eta)u)_\xi, \\ u_t + \dfrac{1}{M(\xi)}uu_\xi + \dfrac{1}{M(\xi)}\left(1-\dfrac{\rho_2}{\rho_1}\right)\eta_\xi = \dfrac{\rho_2}{\rho_1}\dfrac{\sqrt{\beta}}{M(\xi)}\mathcal{T}_h[(1-\eta)u]_{\xi t} + \\ \quad \dfrac{\beta}{1-\eta}\dfrac{1}{3M(\xi)}\left((1-\eta)^3 G_1\right)_\xi + \dfrac{\rho_2}{\rho_1}\dfrac{\beta}{M(\xi)}\left(\dfrac{\eta((1-\eta)u)_{\xi t}}{M(\xi)} + \dfrac{1}{2}((1-\eta)u)_\xi^2\right)_\xi + \\ \quad \dfrac{\beta}{M(\xi)}\dfrac{\rho_2}{\rho_1}\mathcal{T}_h\left[\dfrac{\eta}{M(\xi)}\mathcal{T}_h[(1-\eta)u]_\xi\right]_{\xi t} + \dfrac{\beta}{2M(\xi)}\dfrac{\rho_2}{\rho_1}\left(\left\{\dfrac{1}{M(\xi)}\mathcal{T}_h\left[((1-\eta)u)_\xi\right]\right\}^2\right)_\xi + O(\beta^{\frac{3}{2}}). \end{cases}$$

For the weakly nonlinear regime introduce η^*, u^* such that $\eta = \alpha\eta^*$, $u = \alpha u^*$, with $\alpha = O\left(\sqrt{\beta}\right)$, a typical scaling used for solitary waves. After dropping the asterisks, we have

$$\begin{cases} \eta_t = \dfrac{1}{M(\xi)}[(1-\alpha\eta)u]_\xi, \\ u_t + \dfrac{\alpha}{M(\xi)}uu_\xi + \dfrac{\rho_1-\rho_2}{M(\xi)\rho_1}\eta_\xi = \dfrac{\rho_2}{\rho_1}\dfrac{\sqrt{\beta}}{M(\xi)}\mathcal{T}_h[(1-\alpha\eta)u]_{\xi t} + \dfrac{\beta}{3M(\xi)}\left(\dfrac{u_{\xi t}}{M(\xi)}\right)_\xi + O(\beta^{\frac{3}{2}}). \end{cases} \tag{5.1}$$

When the linear dispersive term $\frac{\beta}{3M(\xi)}\left(\frac{1}{M(\xi)}u_{\xi t}\right)_\xi$ is omitted from the higher-order **weakly nonlinear** model, it has exactly the same form as the lower-order **strongly nonlinear** model (2.1). This might imply that the weakly nonlinear higher-order model should be a good model for moderate amplitude internal waves. Namely, one can work with a simple system of equation and capture accurately the dynamics of waves of moderate amplitude. One of our future goals is to study numerically the regime of validity of the above statements. Furthermore, by having this additional term, that arises from G_1 (in the upper layer modeling), the phase speeds from this higher-order model become substantially more accurate when compared to the exact linear dispersion relation, which is very important in time reversal experiments. This will be shown in the next Subsection. In conclusion, the weakly nonlinear higher-order model might have a large domain of validity, yet to be thoroughly explored in the near future.

5.1. Dispersion relation for the higher-order model

Consider the improved model linearized about the undisturbed, flat bottom, state:

$$\begin{cases} \eta_t = u_\xi, \\ u_t + \left(1-\dfrac{\rho_2}{\rho_1}\right)\eta_\xi = \dfrac{\rho_2}{\rho_1}\sqrt{\beta}\mathcal{T}_h[u]_{\xi t} + \dfrac{\beta}{3}u_{\xi\xi t}. \end{cases}$$

By eliminating η and then letting $u = Ae^{i(kx-\omega t)}$ and $\mathcal{T}_h[e^{ikx}] = i\coth\left(\frac{kh_2}{L}\right)e^{ikx}$, we obtain the dispersion relation

$$\omega^2 = \frac{\left(\frac{\rho_2}{\rho_1}-1\right)k^2}{(1+\frac{\beta}{3}k^2)+\frac{\rho_2}{\rho_1}\sqrt{\beta}k\coth\left(\frac{kh_2}{L}\right)}. \tag{5.2}$$

Observe that we have bounded phase speeds with $\frac{\omega^2}{k^2} \to 0$ as $k \to \infty$. The same is true for the reduced model (2.1) [29]:

$$\omega^2 = \frac{\left(\frac{\rho_2}{\rho_1}-1\right)k^2}{1+\frac{\rho_2}{\rho_1}k\sqrt{\beta}\coth\left(\frac{kh_2}{L}\right)}, \tag{5.3}$$

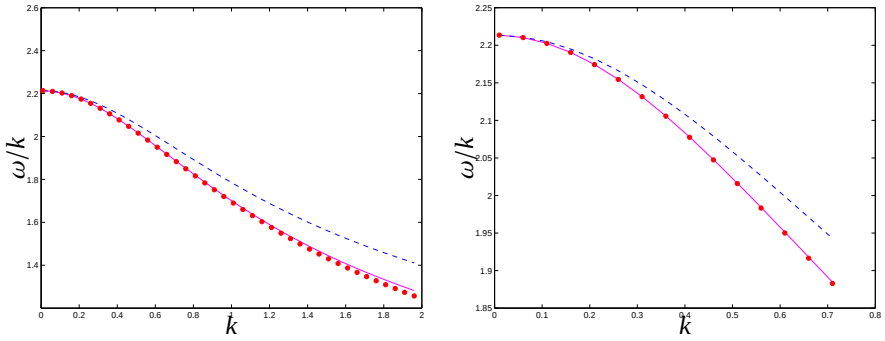

FIG. 5.1. *(a) Phase velocities for $\rho_1 = 1$, $\rho_2 = 2$, $h_1 = 1$, $h_2 = 2$, $\beta = 0.01$. Solid line: full phase velocity, Dotted line: phase velocity for the higher-order model, dashed line: phase velocity for the lower order model; (b) Detail from (a).*

The full dispersion relation, in dimensional form,

$$\omega_f^2 = \frac{g(\rho_2 - \rho_1)k^2}{\rho_1 k \coth(kh_1) + \rho_2 k \coth(kh_2)}, \tag{5.4}$$

arises from the linearized Euler equations [21, 6]. In order to compare the reduced models' dispersion relations, we rewrite (5.2) and (5.3) in dimensional form. The dispersion relation (5.3) becomes

$$\omega_r^2 = \frac{g(\rho_2 - \rho_1)k^2}{\frac{\rho_1}{h_1} + \rho_2 k \coth(kh_2)}.$$

As already stated in [6], the reduced model (2.1) has its upper layer in the shallow water (long wave) regime, which is clearly seen through the limit $\rho_1 k \coth(kh_1) \to \frac{\rho_1}{h_1}$, as $kh_1 \to 0$.

On the other hand, relation (5.2) in dimensional form is

$$\omega_h^2 = \frac{g(\rho_2 - \rho_1)k^2}{\left(\frac{\rho_1}{h_1} + \frac{1}{3}h_1\rho_1 k^2\right) + \rho_2 k \coth(kh_2)}.$$

Notice that both approaches are fully dispersive regarding the bottom layer since the second hyperbolic cotangent is completely retained. This is due to the Hilbert transform on the strip. For the improved shallow water (upper layer) regime (kh_1 near zero), we now obtain the next-order term from the full dispersion relation, namely that

$$\frac{\rho_1}{h_1} kh_1 \coth(kh_1) = \frac{\rho_1}{h_1}\left(1 + \frac{(kh_1)^2}{3} + O\left((kh_1)^4\right)\right),$$

and consequently $\omega_f^2 = \omega_h^2 + O\left((kh_1)^4\right)$, while $\omega_f^2 = \omega_r^2 + O\left((kh_1)^2\right)$. See also Fig. 5.1, where the phase speeds of each of these models are compared. The inclusion of the higher-order pressure term has improved the accuracy of the phase speed over a much wider wavenumber band. This is very important in reflection-transmission problems, as shown by Muñoz and Nachbin [26].

6. Effective equations in a periodic medium

In this section, we present an asymptotic (averaging) theory for the propagation of internal waves over large amplitude rapidly-varying periodic bottom topographies. It is well known that in this regime wave reflection is negligible [32]. Hence, one can write an unidirectional multiscale *ansatz* for the internal waves. As in [32, 16, 7], we consider a weakly non-linear and weakly dispersive regime, with the diverse scales and regimes ordered by a small parameter $\epsilon \ll 1$. In the above references, effective Korteweg-de Vries (KdV) equations were obtained for the free surface wave dynamics. Here we consider the higher-order model (5.1) for weakly nonlinear and weakly dispersive internal waves. Representing the topography, one has the metric term $M(\xi) = m(\xi/\sqrt{\epsilon})$, where $m(\cdot)$ is a 2π-periodic function. Furthermore, the non-linearity and dispersive parameters are scaled as follows: $\alpha = \kappa\epsilon$ and $\beta = (\delta\epsilon)^2$, where κ and δ are constants. Instead of a KdV-type equation, here the leading order effective equation will be of an Intermediate Long Wave-type, which reduces to a Benjamin-Ono-type, when the lower layer is infinitely deep.

6.1. Multi-scale expansions

We look for special asymptotic solutions representing traveling waves. We use the *ansatz*

$$\eta(t,\xi) = \eta_0(\tau,\chi,z) + \sqrt{\epsilon}\eta_1(\tau,\chi,z) + \epsilon\eta_2(\tau,\chi,z) + \cdots, \tag{6.1a}$$

$$u(t,\xi) = u_0(\tau,\chi,z) + \sqrt{\epsilon}u_1(\tau,\chi,z) + \epsilon u_2(\tau,\chi,z) + \cdots, \tag{6.1b}$$

where $\tau = \epsilon t$, $\chi = \xi - vt$, $z = \frac{\xi}{\sqrt{\epsilon}}$, and all the functions are 2π-periodic in z. We note that the propagation velocity v is an unknown constant.

To obtain the corresponding hierarchy of equations, we proceed as customary by using the multi-scale expansions for the unknowns given above and the corresponding expansions of the involved operators. For differentiation operations, these expansions correspond to the chain rule, i.e. $\partial_t \to -v\partial_\chi + \epsilon\partial_\tau$, $\partial_\xi \to \epsilon^{-1/2}\partial_z + \partial_\chi$, but for the non-local operator $\mathcal{T}_h$ we use the following result (see the appendix for a proof). Consider $f^\epsilon(\xi) = g(\xi, \frac{\xi}{\sqrt{\epsilon}})$, where g is 2π-periodic in the second variable and sufficiently regular. Then, as $\epsilon \to 0$, we have the expansion

$$\partial_\xi \mathcal{T}_h[f^\epsilon(\cdot)](\xi) = \partial_\xi \mathcal{T}_h[\langle g(\cdot,\cdot)\rangle](\xi) + \{(\epsilon^{-1/2}\partial_z + \partial_\xi)\mathcal{H}_{per}[g(\xi,\cdot)](z)\}_{z=\frac{\xi}{\sqrt{\epsilon}}} + O(\epsilon^{1/2}), \tag{6.2}$$

where $\langle\cdot\rangle$ and $\mathcal{H}_{per}[\cdot]$ represent, respectively, averaging over the fast variable z, and the standard Hilbert transform of a 2π-periodic function.

6.2. Effective evolution equation

The hierarchy of equations starts at order $\epsilon^{-1/2}$. We have that

$$\eta_{0,z} = 0, \tag{6.3a}$$

$$u_{0,z} = 0. \tag{6.3b}$$

Thus, $\eta_0 = \eta_0(\tau,\chi)$ and $u_0 = u_0(\tau,\chi)$, that is the leading-order terms do not depend on the fast variable z. Our goal is to write closed effective equations for the leading-order wave elevation $\eta_0(\tau,\chi)$.

At order ϵ^0, one gets

$$-vm(z)\eta_{0,\chi} - u_{0,\chi} = u_{1,z} \tag{6.4a}$$

$$-vm(z)u_{0,\chi} - \left(\frac{\rho_2}{\rho_1} - 1\right)\eta_{0,\chi} = \left(\frac{\rho_2}{\rho_1} - 1\right)\eta_{1,z}. \tag{6.4b}$$

After averaging over a period in z, we arrive at

$$v\langle m\rangle\eta_{0,\chi} + u_{0,\chi} = 0, \tag{6.5a}$$

$$v\langle m\rangle u_{0,\chi} + \left(\frac{\rho_2}{\rho_1} - 1\right)\eta_{0,\chi} = 0. \tag{6.5b}$$

To assure the existence of non-trivial solutions, one needs that

$$\det\begin{pmatrix} v\langle m\rangle & 1 \\ \left(\frac{\rho_2}{\rho_1} - 1\right) & v\langle m\rangle \end{pmatrix} = 0,$$

that is

$$v^2 = \frac{\frac{\rho_2}{\rho_1} - 1}{\langle m\rangle^2}. \tag{6.6}$$

As a consequence, we obtain that $u_0(\tau,\chi) = -v\langle m\rangle\eta_0(\tau,\chi)$. To leading order (due to the invariance in χ) η_0 and u_0 are right-travelling waves, as expected.

Introducing the notation, $\bar{u} = \langle u(\cdot)\rangle$, $\tilde{u}(z) = u(z) - \bar{u}$ for 2π-periodic functions in z, subtracting (6.4) and (6.5), and integrating over z we get that

$$\tilde{\eta}_1 = -\frac{v}{\frac{\rho_2}{\rho_1} - 1}\eta_{0,\chi} b(z) \tag{6.7a}$$

$$\tilde{u}_1 = -v u_{0,\chi} b(z) \tag{6.7b}$$

where $b(z)$ solves $db(z)/dz = \tilde{m}(z)$ with the additional condition $\langle b\rangle = 0$.

The equations of order $\epsilon^{1/2}$ read as

$$-vm(z)\eta_{1,\chi} - u_{1,\chi} = u_{2,z} - \kappa(\eta_0 u_0)_z = u_{2,z} \tag{6.8a}$$

$$-vm(z)u_{1,\chi} - \left(\frac{\rho_2}{\rho_1} - 1\right)\eta_{1,\chi} = \left(\frac{\rho_2}{\rho_1} - 1\right)\eta_{2,z} - \frac{\kappa}{2}(u_0^2)_z - v\delta\frac{\rho_2}{\rho_1}\mathcal{H}_{per}[u_0]_{\chi z} = \left(\frac{\rho_2}{\rho_1} - 1\right)\eta_{2,z}. \tag{6.8b}$$

After averaging in z, using (6.7), and noting that $\langle m(z)b(z)\rangle = 0$, we get

$$v\langle m\rangle\bar{\eta}_{1,\chi} + \bar{u}_{1,\chi} = 0, \tag{6.9a}$$

$$v\langle m\rangle\bar{u}_{1,\chi} + \left(\frac{\rho_2}{\rho_1} - 1\right)\bar{\eta}_{1,\chi} = 0, \tag{6.9b}$$

which are compatible when $\bar{u}_{1,\chi} = -v\langle m\rangle\bar{\eta}_{1,\chi}$. Proceeding by integration as before we obtain

$$\tilde{\eta}_2 = \frac{v^2}{\frac{\rho_2}{\rho_1} - 1}\eta_{0,\chi\chi} m_1(z) + \frac{v}{\frac{\rho_2}{\rho_1} - 1}u_{0,\chi\chi} b_1(z) - \frac{v}{\frac{\rho_2}{\rho_1} - 1}\bar{u}_{1,\chi} b(z) \tag{6.10a}$$

$$\tilde{u}_2 = \frac{v^2}{\frac{\rho_2}{\rho_1} - 1}u_{0,\chi\chi} m_1(z) + v\eta_{0,\chi\chi} b_1(z) - v\bar{\eta}_{1,\chi} b(z) \tag{6.10b}$$

where $db_1(z)/dz = b(z)$ with $\langle b_1\rangle = 0$, and $dm_1(z)/dz = m(z)b(z)$ with $\langle m_1\rangle = 0$.

Next, at order ϵ, we have the equations

$$-vm(z)\eta_{2,\chi} - u_{2,\chi} + m(z)\eta_{0,\tau} + \kappa(\eta_0 u_0)_\chi = [u_3 - \kappa(\eta_0 u_1 + u_0\eta_1)]_z, \tag{6.11a}$$

$$\begin{aligned} -vm(z)u_{2,\chi} - \left(\frac{\rho_2}{\rho_1} - 1\right)\eta_{2,\chi} + m(z)u_{0,\tau} + \frac{\kappa}{2}(u_0^2)_\chi = {} & [\left(\frac{\rho_2}{\rho_1} - 1\right)\eta_3 - \kappa u_0 u_1]_z - v\delta\frac{\rho_2}{\rho_1}\mathcal{T}_h[u_{0,\chi\chi}] \\ & - v\delta\frac{\rho_2}{\rho_1}\mathcal{H}_{per}[u_{1,\chi}]_z - \frac{v\delta}{3}[\frac{u_{0,\chi z}}{m(z)}]_z. \end{aligned} \tag{6.11b}$$

Averaging with respect to z, we get that

$$v\langle m\rangle\bar{\eta}_{2,\chi}+\bar{u}_{2,\chi}=\langle m\rangle\eta_{0,\tau}+\kappa(\eta_0u_0)_\chi-v\langle\tilde{m}\tilde{\eta}_{2,\chi}\rangle, \tag{6.12a}$$

$$v\langle m\rangle\bar{u}_{2,\chi}+\left(\frac{\rho_2}{\rho_1}-1\right)\bar{\eta}_{2,\chi}=\langle m\rangle u_{0,\tau}+\frac{\kappa}{2}(u_0^2)_\chi-v\langle\tilde{m}\tilde{u}_{2,\chi}\rangle+v\delta\frac{\rho_2}{\rho_1}\mathcal{T}_h[u_{0,\chi\chi}]. \tag{6.12b}$$

It is easy to establish that $\langle\tilde{m}\tilde{\eta}_{2,\chi}\rangle=\langle\tilde{m}\tilde{u}_{2,\chi}\rangle=0$. Furthermore, since (6.12) are linear in $\bar{\eta}_{2,\chi}$, $\bar{u}_{2,\chi}$ with an associated singular matrix, a non-trivial solution exists when the compatibility condition

$$\left(\frac{\rho_2}{\rho_1}-1\right)\{\langle m\rangle\eta_{0,\tau}+\kappa(\eta_0u_0)_\chi\}-v\langle m\rangle\{\langle m\rangle u_{0,\tau}+\frac{\kappa}{2}(u_0^2)_\chi+v\delta\frac{\rho_2}{\rho_1}\mathcal{T}_h[u_{0,\chi\chi}]\}=0,$$

is satisfied. Finally, after some straightforward calculations, we get the following equation for the leading-order interface elevation η_0,

$$\eta_{0,\tau}-\frac{3\kappa v}{4}(\eta_0^2)_\chi+\frac{\rho_2}{\rho_1}\frac{\delta v}{2\langle m\rangle}\mathcal{T}_h[\eta_{0,\chi\chi}]=0. \tag{6.13}$$

We can rewrite this equation in the t, ξ coordinates, after plugging back the parameters α and β, as

$$\eta_{0,t}+v\eta_{0,\xi}-\frac{3\alpha v}{4}(\eta_0^2)_\xi+\frac{\rho_2}{\rho_1}\frac{\sqrt{\beta}v}{2\langle m\rangle}\mathcal{T}_h[\eta_{0,\xi\xi}]=0. \tag{6.14}$$

This is an *Intermediate Long Wave equation* (ILW) analogous to those considered in the literature for the case of a flat bottom [6, 19, 20]. Actually, all these coincide when we set $\langle m\rangle=1$. Furthermore, within the same order of approximation, we can readily get a regularized version of (6.14)

$$\eta_{0,t}+v\eta_{0,\xi}-\frac{3\alpha v}{4}(\eta_0^2)_\xi-\frac{\rho_2}{\rho_1}\frac{\sqrt{\beta}}{2\langle m\rangle}\mathcal{T}_h[\eta_{0,\xi t}]=0. \tag{6.15}$$

The influence of the bottom appears in the effective ILW equation only through the average metric coefficient, which also is present in $v=\langle m\rangle^{-1}\sqrt{(\rho_2-\rho_1)/\rho_1}$. In the limit where $h\to\infty$, one gets from (6.14) the Benjamim-Ono equation (BO) and from (6.15) the regularized BO equation. Of course, in this case, the bottom is not felt anymore, but it indicates the connection between these important equations. It is also worth noticing that (6.14) and (6.15) admit a one parameter family of solitary wave solutions.

7. Conclusions

We derived a higher-order, strongly nonlinear, one-dimensional Boussinesq-type model for the evolution of internal waves in a two-layer system. The system has variable coefficients expressing large changes in the bathymetry. The presence of the higher-order term, in the pressure coupling between layers, will be further investigated concerning the interaction of internal waves and large amplitude bathymetric variations. The bathymetry has an arbitrary, not necessarily smooth, profile.

A simpler model is considered, namely a weakly nonlinear higher-order system, and shown to have very good dispersive properties. It was also studied through an averaging analysis, for internal waves in the presence of large amplitude, rapidly varying, periodic bathymetries. The averaging strategy leads to an effective ILW equation.

Models with a higher-order pressure approximation are the objective of ongoing research and future numerical experimentation, in particular, having solitary waves travel over a disordered topography. A future goal is the careful study of regimes where the apparent diffusion and time-reversal of internal waves can be observed [10, 11, 12, 15].

Appendix A. Multi-scale expansion of the non-local operator.

In this appendix, we present an asymptotic expansion involving the Hilbert operator on a strip of width h

$$\mathcal{T}_h[f](\xi) = \fint dk e^{ik\xi}(i\coth(hk))\hat{f}(k), \tag{A.1}$$

where the Fourier transform $\hat{f}$ is given as

$$\hat{f}(k) = \frac{1}{2\pi}\int d\xi e^{-ik\xi} f(\xi).$$

Let $f^\epsilon(\xi) = g(\xi, \frac{\xi}{\sqrt{\epsilon}})$, where g is 2π-periodic in the second variable. Our aim is to obtain a multi-scale expansion for $\partial_\xi \mathcal{T}_h[f^\epsilon(\cdot)](\xi)$ as $\epsilon \to 0$. We have the following result.

Proposition A.1. *Let $f^\epsilon(\xi) = g(\xi, \frac{\xi}{\sqrt{\epsilon}})$ be such that for $p > 3/2$, $s > 3/2 + q$, $q > 0$,*

$$\int dk \sum_{m\neq 0}(1+k^2)^s |m|^{2p} |(\mathcal{F}g)(k,m)|^2 < \infty.$$

The (full) Fourier transform $(\mathcal{F}g)$ of the function $g(\xi,z)$ is given by

$$(\mathcal{F}g)(k,m) = \frac{1}{(2\pi)^2}\int d\xi \int_0^{2\pi} dz e^{-i(k\xi+mz)} g(\xi,z), \qquad k\in\mathbb{R},\ m\in\mathbb{Z}.$$

Then, as $\epsilon \to 0$, we have the following asymptotic expansion

$$\partial_\xi \mathcal{T}_h[f^\epsilon(\cdot)](\xi) = \partial_\xi \mathcal{T}_h[\langle g(\cdot,\cdot)\rangle](\xi) + \left\{(\epsilon^{-1/2}\partial_z + \partial_\xi)\mathcal{H}_{per}[g(\xi,\cdot)](z)\right\}_{z=\frac{\xi}{\sqrt{\epsilon}}} + r_\epsilon(\xi), \tag{A.2}$$

where $\langle\cdot\rangle$ represents the mean value of a 2π-periodic function, and $r_\epsilon(\xi) = O(\epsilon^{q/2})$, uniformly in ξ. Also $\mathcal{H}_{per}[\cdot]$ is the Hilbert transform for 2π-periodic functions.

We note that in the context of calculating the effective evolution equation, we require $q \geq 1$.

Proof. Using the Fourier representation

$$g(\xi,z) = \int dk \sum_{m\in\mathbb{Z}} e^{i(k\xi+mz)}(\mathcal{F}g)(k,m),$$

together with equation (A.1), we get that

$$\begin{aligned}\partial_\xi \mathcal{T}_h[f^\epsilon(\cdot)](\xi) &= \int dk \sum_{m\in\mathbb{Z}} e^{i(k+\frac{m}{\sqrt{\epsilon}})\xi} i(k+\frac{m}{\sqrt{\epsilon}}) i\coth[h(k+\frac{m}{\sqrt{\epsilon}})](\mathcal{F}g)(k,m)\\ &= \partial_\xi \mathcal{T}_h[\langle g(\cdot,\cdot)\rangle](\xi) + \int dk \sum_{m\neq 0} e^{i(k+\frac{m}{\sqrt{\epsilon}})\xi} i(k+\frac{m}{\sqrt{\epsilon}})\\ &\quad \times i\coth[h(k+\frac{m}{\sqrt{\epsilon}})](\mathcal{F}g)(k,m).\end{aligned}$$

Recall that for the periodic function $f(z)$, the Hilbert transform is given as

$$\mathcal{H}_{per}[f(\cdot)](z) = \sum_{m\neq 0} e^{imz}(i\,\mathrm{sgn}(m))\hat{f}(m),$$

where $\hat{f}(m)$ represents the Fourier coefficients of $f(z)$. Consequently, to establish the result, one needs to estimate

$$r_\epsilon(\xi) = \int dk \sum_{m\neq 0} e^{i(k+\frac{m}{\sqrt{\epsilon}})\xi} i(k+\frac{m}{\sqrt{\epsilon}}) i\left\{\coth[h(k+\frac{m}{\sqrt{\epsilon}})] - \mathrm{sgn}(m)\right\}(\mathcal{F}g)(k,m). \tag{A.3}$$

First, fix a such that $0<a<1$ and consider that $|k|\leq\epsilon^{-a/2}$. For $m\neq 0$ and $\epsilon<1$, small enough, we have that $|k+\frac{m}{\sqrt{\epsilon}}|>\frac{1}{2\sqrt{\epsilon}}$ and $\mathrm{sgn}(m)=\mathrm{sgn}(k+\frac{m}{\sqrt{\epsilon}})$. Consequently, we get that $|\coth[h(k+\frac{m}{\sqrt{\epsilon}})]-\mathrm{sgn}(m)|<c_1\exp(-\frac{h}{2\sqrt{\epsilon}})$, and the low frequency part of the integral (A.3) (using the cutoff frequency $\epsilon^{-a/2}$) can be readily estimated. In fact, we can decompose that integral into two integrals, which correspond to the two terms of the factor $k+\frac{m}{\sqrt{\epsilon}}$ in (A.3).

We present here the estimate for one of these integrals. For the other one, we proceed in a similar way. Using the Cauchy-Schwarz inequality, we get the following estimate

$$
\begin{aligned}
I_1(\epsilon) &= \Big|\int_{-\epsilon^{-a/2}}^{\epsilon^{-a/2}} dk \sum_{m\neq 0} e^{i(k+\frac{m}{\sqrt{\epsilon}})\xi}\frac{im}{\sqrt{\epsilon}} i\{\coth[h(k+\frac{m}{\sqrt{\epsilon}})]-\mathrm{sgn}(m)\}(\mathcal{F}g)(k,m)\Big| \\
&\leq \frac{c_1}{\sqrt{\epsilon}}\exp(-\frac{h}{2\sqrt{\epsilon}})\int_{-\epsilon^{-a/2}}^{\epsilon^{-a/2}} dk\sum_{m\neq 0}|m(\mathcal{F}g)(k,m)| \\
&\leq \frac{c_1}{\sqrt{\epsilon}}\exp(-\frac{h}{2\sqrt{\epsilon}})\int dk\sum_{m\neq 0}\frac{1}{|m|^{p_1-1}(1+k^2)^{s_1/2}}|m|^{p_1}(1+k^2)^{s_1/2}(\mathcal{F}g)(k,m)| \\
&\leq \frac{c_1}{\sqrt{\epsilon}}\exp(-\frac{h}{2\sqrt{\epsilon}})\Big(\int dk\sum_{m\neq 0}\frac{1}{|m|^{2(p_1-1)}(1+k^2)^{s_1}}\Big)^{1/2} \\
&\quad\times\Big(\int dk\sum_{m\neq 0}|m|^{2p_1}(1+k^2)^{s_1}|(\mathcal{F}g)(k,m)|^2\Big)^{1/2}.
\end{aligned}
$$

If both integrals in the last inequality above are finite, then $I_1(\epsilon)\to 0$ faster than any power of ϵ as $\epsilon\to 0$. For the first integral factor to be finite, it is necessary that $p_1>3/2$ and $s_1>1/2$. The second factor is finite by hypothesis. Thus, taking $p_1=p$ and $s_1=s$, namely, taking the same bounds as in the proposition's statement, one gets that $I_1(\epsilon)\leq O(\epsilon^{q/2})$ as $\epsilon\to 0$.

Now, we have to estimate the high frequency part of integral (A.3). Observe that the function $\coth(x)$ is bounded in any set not containing a neighborhood of 0, while near the origin the function $x\coth(x)\to 1$ as $x\to 0$. Consequently, there are constants $c_2>1/h$, $c_3>1$ such that

$$
\Big|(k+\frac{m}{\sqrt{\epsilon}})\{\coth[h(k+\frac{m}{\sqrt{\epsilon}})]-\mathrm{sgn}(m)\}\Big|\leq c_2+c_3(|k|+\Big|\frac{m}{\sqrt{\epsilon}}\Big|),\qquad k\in\mathbb{R},m\in\mathbb{Z}. \tag{A.4}
$$

Thus, we need to estimate the three high frequency integrals corresponding to each term in the right-hand-side of the inequality above.

We proceed to estimate one of these integrals, namely the one that produces the most restrictive bound on s. The other integrals can be dealt with in a similar way. Assume initially

that $p_2 > 3/2$, $s_2 > 1/2$, then we have the following estimates

$$
\begin{aligned}
I_2(\epsilon) &= \int_{\{|k|>\epsilon^{-a/2}\}} dk \sum_{m\neq 0} (c_3 \Big| \frac{m}{\sqrt{\epsilon}} \Big|) |(\mathcal{F}g)(k,m)| \\
&\leq \frac{c_3}{\sqrt{\epsilon}} \int_{\{|k|>\epsilon^{-a/2}\}} dk \sum_{m\neq 0} \frac{1}{|m|^{p_2-1}|k|^{s_2}} |m|^{p_2} (1+k^2)^{s_2/2} |(\mathcal{F}g)(k,m)| \\
&\leq \frac{c_3}{\sqrt{\epsilon}} \Big(\int_{\{|k|>\epsilon^{-a/2}\}} dk \sum_{m\neq 0} \frac{1}{|m|^{2(p_2-1)}|k|^{2s_2}} \Big)^{1/2} \\
&\qquad \times \Big(\int dk \sum_{m\neq 0} |m|^{2p_2} (1+k^2)^{s_2} |(\mathcal{F}g)(k,m)|^2 \Big)^{1/2} \\
&\leq \frac{c_3'}{\sqrt{\epsilon}} \Big(\int_{\epsilon^{-a/2}}^{\infty} \frac{dk}{k^{2s_2}} \Big)^{1/2} \Big(\sum_{m\neq 0} \frac{1}{|m|^{2(p_2-1)}} \Big)^{1/2} \\
&\qquad \times \Big(\int dk \sum_{m\neq 0} |m|^{2p_2} (1+k^2)^{s_2} |(\mathcal{F}g)(k,m)|^2 \Big)^{1/2} \\
&\leq c_3'' \epsilon^{[a(2s_2-1)/4-1/2]} \Big(\int dk \sum_{m\neq 0} |m|^{2p_2} (1+k^2)^{s_2} |(\mathcal{F}g)(k,m)|^2 \Big)^{1/2}.
\end{aligned}
$$

This last integral is finite by hypothesis, so we require that $a(2s_2-1)/4 - 1/2 = q/2$ (i.e. $s_2 = 1/2 + (q+1)/a$). Then one gets that $I_2(\epsilon) = O(\epsilon^{q/2})$ as $\epsilon \to 0$. However, as a function of a, $s_2(a)$ maps $a \in (0,1)$ onto $(3/2+q, \infty)$. Therefore, having imposed earlier that $a \in (0,1)$, the desired estimate $I_2(\epsilon) = O(\epsilon^{q/2})$ will be always achieved once $s_2 = s > 3/2 + q$. The value of a is connected to s and therefore depends on the regularity of the function g.

□

REFERENCES

[1] W. Artiles and A. Nachbin. Nonlinear evolution of surface gravity waves over highly variable depth, Phys. Rev. Lett. 93:234501 (2004).

[2] T. B. Benjamin. Internal waves of permanent form of great depth, J. Fluid Mech. 9:559–592 (1967).

[3] R. Camassa and C. D. Levermore. Layer-mean quantities, local conservation laws, and vorticity, Phys. Rev. Lett. 78:650–653 (1997).

[4] W. Choi and R. Camassa. Long internal waves of finite amplitude, Phys. Rev. Lett. 77:1759–1762 (1996).

[5] W. Choi and R. Camassa. Weakly nonlinear internal waves in a two-fluid system. J. Fluid Mech. 313:83–103 (1996).

[6] W. Choi and R. Camassa. Fully nonlinear internal waves in a two-fluid system. J. Fluid Mech. 396:1–36 (1999).

[7] W. Craig and C. Sulem. Numerical Simulation of Gravity Waves. J. Comp. Phys. 108:73-83 (1993).

[8] W. Craig, P. Guyenne, D.P. Nicholls, and C. Sulem. Hamiltonian long wave expansions for water waves over a rough bottom, Proc. R. Soc. A, 461:839–873 (2005).

[9] R. E. Davis and A. Acrivos. Solitary internal waves in deep water. J. Fluid Mech. 29:593–607 (1967).

[10] J. P. Fouque, J. Garnier and A. Nachbin. Shock structure due to stochastic forcing and the time reversal of nonlinear waves. Physica D 195:324–346 (2004).

[11] J. P. Fouque, J. Garnier and A. Nachbin. Time reversal for dispersive waves in random media. SIAM J. App. Math. 64:1810–1838 (2004).

[12] J. P. Fouque, J. Garnier, J. C. Muñoz and A. Nachbin. Time reversing solitary waves. Phys. Rev. Lett. 92:094502 (2004).

[13] J. Garnier and A. Nachbin. The eddy viscosity for time reversing waves in a dissipative environment. Phys. Rev. Lett. 93:154501 (2004).

[14] J. Garnier and A. Nachbin. The eddy viscosity for gravity waves propagating over turbulent surfaces. Phys. of Fluids. 18:055101 (2006).

[15] J. Garnier, J. C. Muñoz and A. Nachbin. A Effective behavior of solitary waves over random topography. SIAM Multiscale Model. Simul. 6:995–1025 (2007).

[16] J. Garnier, R. Kraenkel and A. Nachbin. An optimal Boussinesq model for shallow water wave-microstructure interaction. Phys. Rev. E. 76:046311 (2007).
[17] A. E. Green and P. M. Naghdi. A derivation of equations for wave propagation in water of variable depth. J. of Fluid Mech. 78:237–246 (1976).
[18] T.-C. Jo and W. Choi. Dynamics of strongly nonlinear internal solitary waves in shallow water. Stud. Appl. Math. 109:205–227 (2002).
[19] R. I. Joseph. Solitary waves in finite depth fluid. J. Phys. A 10L225–L227 (1977).
[20] T. Kubota, D. Ko and L. Dobbs. Propagation of weakly nonlinear internal waves in a stratified fluid of finite depth. AIAA J. Hydrodynamics 12:157–165 (1978).
[21] H. Lamb, Hydrodynamics, Dover, 1932.
[22] Y. Matsuno. Nonlinear evolutions of surface gravity waves on fluid of finite depth. Phys. Rev. Lett. 69:609–611 (1992).
[23] P. Milewski, E. Tabak, C. Turner, R. Rosales and F. Menzaque. Nonlinear stability of two-layer flows. Comm. Math. Sci. 2:427–442 (2004).
[24] J. C. Muñoz and A. Nachbin. Dispersive wave attenuation due to orographic forcing. SIAM J. Appl. Math. 64:977–1001 (2004).
[25] J. C. Muñoz and A. Nachbin. Stiff microscale forcing and solitary wave refocusing. SIAM Multiscale Model. Simul. 3:680–705 (2005).
[26] J. C. Muñoz and A. Nachbin. Improved Boussinesq-type equations for highly-variable depths. IMA J. App. Math. 71:600–633 (2006).
[27] A. Nachbin. A terrain-following Boussinesq system. SIAM J. Appl. Math. 63:905–922 (2003).
[28] A. Nachbin and K. Solna. Apparent diffusion due to orographic microstructure in shallow waters. Phys. Fluids. 15:66–77 (2003).
[29] A. Ruiz de Zárate and A. Nachbin. A Reduced Model for internal waves interacting with topography at intermediate depth. Comm. Math. Sci. 6:385-396 (2008).
[30] A. Ruiz de Zárate. A reduced model for internal waves interacting with submarine structures at intermediate depth. PhD Thesis, IMPA, (2007).
http://www.preprint.impa.br/FullText/008_Thu_Feb__7_16_25_14_BRDT_2008/serie_C_55A.pdf.
[31] H. Ono. Algebraic solitary waves in stratified fluids. J. of the Phys. Soc. of Japan. 39:1082–1091 (1975).
[32] R. R. Rosales and G. C. Papanicolaou. Gravity waves in a channel with a rough bottom. Stud. Appl. Math. 68:89–102 (1983).
[33] C. H. Su and C. S. Gardner. Korteweg-de Vries Equation and Generalizations. III. Derivation of the Korteweg-de Vries Equation and Burgers Equation. J. of Math. Phys. 10:536–539 (1969).
[34] T. Y. Wu. Long waves in ocean and coastal waters. J. of the Eng. Mech. Div. ASCE. 107:501–522 (1981).